fishes

MDPI

Article

Investigations on Target Strength Estimation Methods: A Case Study of Chub Mackerel (*Scomber japonicus*) in the Northwest Pacific Ocean

Zhenhong Zhu [1,2,3], Jianfeng Tong [1,4,5,*], Minghua Xue [1], Chuhan Qiu [1], Shuo Lyu [1] and Bilin Liu [1,4,5]

[1] College of Marine Living Resource Sciences and Management, Shanghai Ocean University, Shanghai 201306, China; zhuzhenhong1996@163.com (Z.Z.); d220200065@st.shou.edu.cn (M.X.); q15836082195@163.com (C.Q.); 13624518054@163.com (S.L.); bl-liu@shou.edu.cn (B.L.)
[2] Wuxi Fisheries College, Nanjing Agricultural University, Wuxi 214081, China
[3] Key Laboratory of Freshwater Fisheries and Germplasm Resources Utilization, Ministry of Agriculture and Rural Affairs, Freshwater Fisheries Research Center, Chinese Academy of Fishery Sciences, Wuxi 214081, China
[4] National Engineering Research Center for Oceanic Fisheries, Shanghai 201306, China
[5] Key Laboratory of Sustainable Exploitation of Oceanic Fisheries Resources, Ministry of Education, Shanghai 201306, China
* Correspondence: jftong@shou.edu.cn

Abstract: Target strength (TS) is an acoustic property of individual marine organisms and a critical factor in acoustic resource assessments. However, previous studies have primarily focused on measuring TS at narrowband, typical frequencies, which cannot meet the requirements of broadband acoustic technology research. Additionally, for marine fish, conducting in situ TS measurements is challenging due to environmental constraints. Rapidly freezing and preserving fish samples for transfer to the laboratory is a common method currently used. However, the impact of freezing preservation during transportation on the swimbladder morphology and TS of swimbladder-bearing fish remains unclear. This study investigated the differences in swimbladder morphology and TS of Chub mackerel (*Scomber japonicus*) before and after freezing. Then, we compared different TS measurement methods through ex situ TS measurements (45–90 kHz, 160–260 kHz) and the Kirchhoff-ray mode model (KRM) simulations (1–300 kHz) and studied the broadband scattering characteristics of Chub mackerel based on the KRM model. The results showed that the morphology of the swimbladder was reduced after freezing, with significant changes in swimbladder height and volume. However, the trends of TS were not consistent and the changes were small. The difference between the KRM model and ex situ measurements was -0.38 ± 1.84 dB, indicating good applicability of the KRM. Based on the KRM results, the TS exhibited significant directivity, with fluctuations gradually decreasing and stabilizing as frequency increased. In the broadband mode, the relationship between TS and body length (L) of Chub mackerel was $TS = 20\log(L) - 66.76$ ($30 > L/\lambda > 10$). This study could provide a reference for acoustic resource estimation and species identification of Chub mackerel in the Northwest Pacific Ocean.

Keywords: Chub mackerel; swimbladder morphology; target strength; broadband scattering response; acoustic resource estimation

Key Contribution: The study examined the changes in the swimbladder morphology and TS before and after freezing, compared the differences between ex situ measurements and model estimates, and obtained the broadband scattering characteristics of Chub mackerel.

check for updates

Citation: Zhu, Z.; Tong, J.; Xue, M.; Qiu, C.; Lyu, S.; Liu, B. Investigations on Target Strength Estimation Methods: A Case Study of Chub Mackerel (*Scomber japonicus*) in the Northwest Pacific Ocean. *Fishes* **2024**, *9*, 307. https://doi.org/10.3390/fishes9080307

Academic Editor: Konstantinos Tsagarakis

Received: 8 June 2024
Revised: 13 July 2024
Accepted: 1 August 2024
Published: 3 August 2024

1. Introduction

The fisheries acoustic technology based on echosounders aims to conduct remote sensing detection of fishery resources and even marine ecosystems without biological and

environmental damage, providing fishery-independent scientific data [1,2]. Compared to biological sampling methods, fisheries acoustic technology can provide vertical profile data for detailed analysis of water layers, offering much broader survey coverage [3]. One of the main focuses of fisheries acoustic research is converting acoustic data into biomass data to assess the abundance of target species in the survey area. The key parameter affecting the accuracy of biomass data is target strength (TS; dB re 1 m^2), which represents the ability of an individual organism to reflect sound waves [4]. Additionally, with the widespread use of broadband scientific echosounders that can transmit a wide and continuous frequency range, acoustic data resolution, and signal-to-noise ratio (SNR) have been increased, significantly improving the ability to target classification based on backscatter spectra [5,6]. The backscatter spectrum of a single individual, which is the variation of TS at the continuous frequency ($TS(f)$), correlates with the backscattering from schools ($Sv(f)$) of the same species: $Sv(f) = TS(f) + 10\log\rho$, where ρ is the biomass density in schools [7]. Therefore, to achieve species identification based on broadband acoustic technology, it is first necessary to study the spectral characteristics of individual target strength.

Fish TS is influenced by various factors, including fish species, acoustic frequency, presence or absence of a swimbladder, body length, and swimming posture [8–11]. For swimbladder-bearing fish, the density contrast between the swimbladder and the body tissue greatly impacts the acoustic pulse, with up to 95% of the backscatter attributable to the swimbladder [8]. The study on Argentine anchovy (*Engraulis anchoita*) TS by Madirolas et al. [12], based on the Prolate Spheroidal Model (PSM), indicated that the variation in fish TS at different incident angles was consistent with the TS variation of the swimbladder, while the TS of the fish body remained low. The study by Li et al. [13] on Thorn fish (*Terapon jarbua*) using the Kirchhoff-ray mode (KRM) also corroborated this perspective. Changes in swimbladder morphology can significantly influence TS and lead to considerable differences in biomass estimates [14,15].

Current research on TS estimation mainly includes direct measurement methods, such as in situ [16,17] and ex situ measurements [18–20], as well as acoustic scattering model estimation methods based on morphological parameters [21–23]. In situ measurements can obtain TS data in the natural state, but are limited by the field environment, interference from other organisms, and the inability to control the length distribution of the fish, making it challenging to accurately establish TS–length relationships [24]. Ex situ measurements are conducted by setting up experimental environments and using methods such as net cages and tethering to measure fish echo information. Although this approach allows for linking TS data with fish length, it alters the natural state of the fish. Using samples that have been anesthetized or frozen may lead to changes in their morphology, potentially causing deviations in TS measurements [25]. While direct measurement experiments can better reflect the TS under real conditions, both in situ and ex situ measurements present significant challenges in data collection, and sample size is also a crucial factor limiting the accuracy of the obtained TS data [26]. Acoustic scattering models approximate the geometric shape based on the morphological characteristics of the fish and estimate TS using scattering theory. This approach facilitates the study of TS variations under different influencing factors [9]. However, the accuracy of the models is limited by the precision of geometric measurements. Additionally, each model has its advantages and limitations, and the choice of model depends on the target shape and specific requirements [27]. Generally, as the accuracy of models continues to improve, research on TS based on acoustic scattering models has been increasing. However, the comparison between actual measurements and model estimates remains noteworthy. Hazen et al. [28] compared the ex situ TS measurements with the predictions of the backscatter model, examining the differences between the two methods in terms of fish length, tilt, depth, and frequency. Peña et al. [29] constructed an accurate fish body morphology based on MRI scan results and compared it with the standard TS obtained from ex situ experiments. Numerous studies have demonstrated the differences and applicability between various TS measurement methods.

In conducting research related to the TS of marine fish, the complexity of the environment and the interference from various factors affecting TS make in situ TS measurements challenging. Therefore, ex situ measurements in laboratory or acoustic scattering model estimations are often used instead [30,31]. Both of these methods require transferring biological samples from the survey area to the laboratory, often facing long-term preservation challenges. Additionally, for swimbladder-bearing fish, it is even more important to maintain the integrity of the swimbladder morphology. Different preservation methods may lead to structural changes in the fish body or compression of the swimbladder, resulting in variations in TS. Sobradillo et al. [15] placed the samples in liquid nitrogen and then stored them frozen at −15 °C, but obtaining sufficient liquid nitrogen on board was more difficult. Rapid freezing of fresh samples preserved in a seawater-filled sampling device is the current common method [32,33], but attention should be paid to the differences in fish swimbladder morphology before and after freezing. Currently, there is a lack of research on the impact of different sample preservation methods on swimbladder morphology.

The confluence of cold and warm currents in the Northwest Pacific Ocean creates abundant fishery resources, making it one of the highest-yielding marine fishing areas in the world [34]. As a significant pelagic fishery resource, Chub mackerel is widely distributed and possesses high economic value. It holds an important position among the various fishery resources in the Northwest Pacific Ocean and is under the jurisdiction of the North Pacific Fisheries Commission (NPFC) [35]. With the continuous development of global fisheries, the exploitation of Chub mackerel resources has been intensifying. According to the NPFC statistics, there has been a general declining trend in catches from the 1980s to the present, which has attracted closer attention from the NPFC and related researchers [36]. As early as 2015, the NPFC listed Chub mackerel as a priority species for management, and a working group was established to carry out research on the status of Chub mackerel stocks and conservation management. However, the assessment of Chub mackerel resources has not yet been completed [37]. The International Council for the Exploration of the Sea (ICES), the Commission for the Conservation of Antarctic Marine Living Resources (CCAMLR), and other organizations have established relevant acoustic research working groups. They utilize acoustic technology to provide references for the assessment and management of fisheries resources. However, the acoustic method has not been widely applied in the Northwest Pacific Ocean.

Target strength (TS) is a crucial aspect of fisheries acoustics research, directly affecting the accuracy of fishery resource assessments. The primary objectives of this study are: (a) to investigate the changes in swimbladder morphology and their impact on TS caused by freezing preservation of fish samples, by measuring the morphological parameters of the swimbladder and fish body before and after freezing; (b) to compare the differences between ex situ TS measurements and KRM model results, validating the applicability of the KRM model for TS measurement in Chub mackerel; and (c) to obtain the broadband scattering response characteristics and the relationship between TS and body length at typical frequencies for Chub mackerel. This study aims to provide fundamental data for the acoustic resource assessment of Chub mackerel and to support species identification research based on broadband acoustic technology, thereby promoting the application of fisheries acoustic technology in the management of fishery resources in the Northwest Pacific.

2. Materials and Methods

2.1. Biological Sample Collection

Fish samples were collected from a scientific survey of pelagic fishery resources in the Northwest Pacific Ocean (34–45° N, 147–165° E), carried by the scientific research vessel "Songhang" from 15 June to 30 July 2022. The study area was located at the confluence of the Kuroshio warm current and the Oyashio cold current, which was characterized by a rich aggregation of biological resources [38,39]. The survey deployed a four-panel fine mesh mid-water trawl, with primary dimensions of 434 × 97.1 m and a 40 mm stretch cod-end mesh, structured as a single bag. The deployment and position of the trawl, as well

as the net opening size and other relevant details, were closely monitored and recorded using a trawl sounder [40]. Within the area, a total of 36 biological sampling stations were established. Each trawling operation lasted approximately 1.5 h, with an average depth of 44.98 ± 13.74 m. The vessel speed was approximately 4–5 knots.

At all sampling stations, Chub mackerel catches were randomly selected as active or undamaged and transferred to sampling bottles filled with seawater. A portion of the samples was randomly chosen to be dissected in the onboard biological laboratory, while the remainder was placed in the −20 °C freezer for rapid freezing and preservation, intended for research after the return voyage.

2.2. Morphological Measurements

The morphological parameters measured for each sample are shown in Figure 1, including fish body length (fbl), body width (fbw), body height (fbh), swimbladder length (sbl), swimbladder width (sbw), swimbladder height (sbh), and swimbladder tilt angle. The swimbladder tilt angle is defined as the angle between the central axes of the fish body and swim bladder.

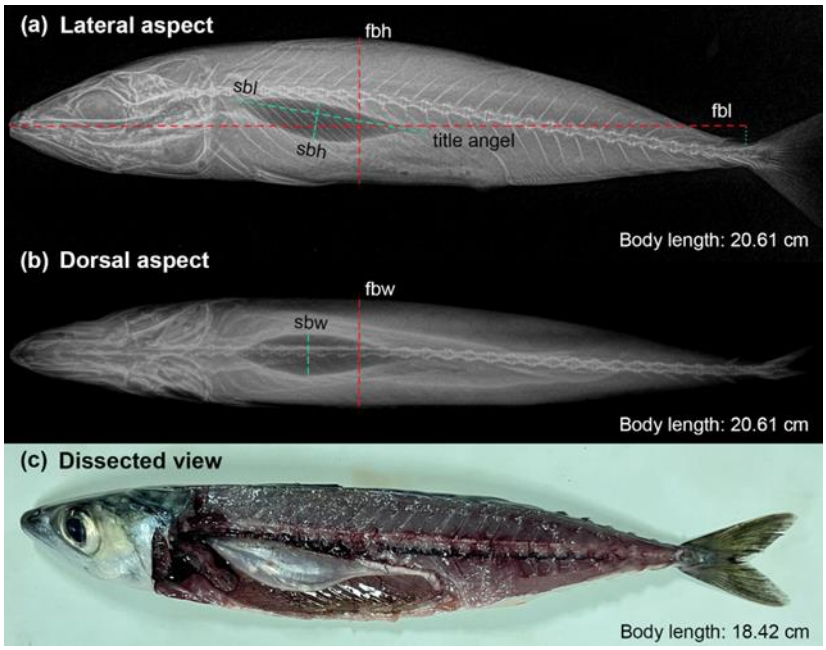

Figure 1. Morphological measurements of Chub mackerel on (**a**) lateral X-ray image, (**b**) dorsal X-ray image, and (**c**) dissected view image. The red lines indicate measurements of the fish body, and the green lines indicate measurements of the swimbladder.

Morphological characteristics of Chub mackerel body and swimbladder were obtained by dissection and X-ray imaging system, respectively. Due to the lack of measurement equipment onboard, swimbladder morphological parameters were obtained through dissection. The abdomen, lateral muscles, and stomach contents were removed, then fish body and swimbladder morphology were measured using a vernier caliper, as shown in Figure 1c. After the survey, morphological images of the fish body and swimbladder were acquired using an X-ray imaging system in the laboratory. The seawater frozen samples were thawed naturally in cold seawater for about 12 h to minimize any damage on swimbladder shape [32,33]. The defrosted samples with better preserved appearance were selected for measuring body length and weight. Subsequently, each sample was scanned with X-rays from both lateral and dorsal aspects to obtain contour images of the fish body and swimbladder (Figure 1a,b). Image files from X-ray scans were processed using Photoshop (V2021, Adobe Systems Inc., San Jose, CA, USA). The measuring scale was constructed based on the fish body length measurements. The fish was appropriately

rotated to ensure a level posture, and the grayscale threshold was adjusted to improve the contrast between the swimbladder and the fish body, facilitating accurate identification of the swimbladder boundary. Then manual measurements of the morphological parameters of both the fish body and swimbladder were performed.

According to the measurement results, we conducted approximate calculations of the volume and the cross-sectional area from the dorsal direction of the fish body and swimbladder [41]:

$$V = 4\pi/3 \cdot (l_a/2) \cdot (l_b/2) \cdot (l_c/2) \quad (1)$$

$$S = \pi \cdot (l_a/2) \cdot (l_b/2) \quad (2)$$

where l_a, l_b, and l_c, respectively, represent the length, width, and height of the fish body or swimbladder (cm).

The equivalent spherical radius [33] was estimated following the equation:

$$r = (sbl \cdot sbw \cdot sbh)^{1/3} \quad (3)$$

where sbl, sbw, and sbh, respectively, represent the length, width, and height of the swimbladder (cm).

As a vital organ controlling the buoyancy, the swimbladder typically follows a simple allometric growth pattern. It can be represented using the linear relationship between the equivalent spherical radius and body length:

$$log_{10}L = a + q \cdot log_{10}r \quad (4)$$

where L is the body length (cm), a is a constant, and q is the allometric exponent. When $0 < q < 1$, it is negative allometric growth, when $q = 1$, it is isometric growth, and when $q > 1$, it is positive allometric growth [42].

2.3. Acoustic Backscattering Model

Based on the morphological parameters measured by the X-ray imaging system of the fish body and swimbladder, the Kirchhoff-Ray mode model (KRM) [43] was constructed to simulate the acoustic scattering characteristics of different fish samples. The KRM model approximates the fish body and swimbladder as a series of contiguous cylinders filled with liquid and gas. It calculates the scattering of each part and then coherently sums them to generate the TS result of individual fish [2]. The typical acoustic parameters of fish and water required by the model used were sourced from the research of Clay and Horne [44], listed in Table 1. Using the KRM model, the backscattering cross-sections (σ_{bs}) of fish at different frequencies and incident angles of sound waves were obtained, which is a linear representation of the TS. The frequency range was 1–300 kHz, encompassing the common frequencies used for resource surveys. Since the KRM model becomes inaccurate at a high off-broadside angle [21], the incident wave was limited to the range of 40° to 140°, where the angle greater than 90° is head down, and less than 90° is head up. Referring to the research of Tong et al. [45], the KRM model was established in MATLAB (R2018a, MathWorks Inc., Natick, MA, USA).

Table 1. Acoustic parameters used in the KRM model.

Model Parameters	Values	Unit
Density of sea water	1030	kg/m^3
Density of fish body	1070	kg/m^3
Density of swimbladder	1.24	kg/m^3
Sound speed in sea water	1490	m/s
Sound speed in fish body	1570	m/s
Sound speed in swimbladder	345	m/s

2.4. Ex Situ Target Strength Measurements

The ex situ TS measurements were conducted in an anechoic tank (length, 15 m; width, 7 m; depth, 6 m) at the Fishery Machinery and Instrument Research Institute, Chinese Academy of Fishery Sciences, in October 2023. The measurement system is shown in Figure 2. Two transducers were installed on one side of the tank near the wall, with Mechanism A used to control their position and switch between the transducers. Fish were tethered on the other side of the tank using fishing lines and connected to Mechanism B. The metal rod was suspended below the fish to maintain its stable posture. The distance between the fish and transducers was 7 m, and they were positioned at the same depth of 2 m underwater, with the dorsal side of the fish facing the working transducer. Mechanism B controlled the horizontal rotation of the fish, with angles ranging from 40° (head up) to 140° (head down) at 5° intervals. After each angle rotation, the fish was centered in the beam and held still for approximately 5 s to stabilize its posture, following which echo data were recorded for 5 s. Corresponding to different transducers, the fish underwent the same angle rotations individually. Before and after the experiment, measurements of water temperature and salinity were conducted for transducer calibration. Prior to the start of measurements, the fish were slowly thawed for about 12 h. Then X-ray images were taken, and fish samples undamaged in swimbladder morphology were selected, along with measurements of fish body length and weight.

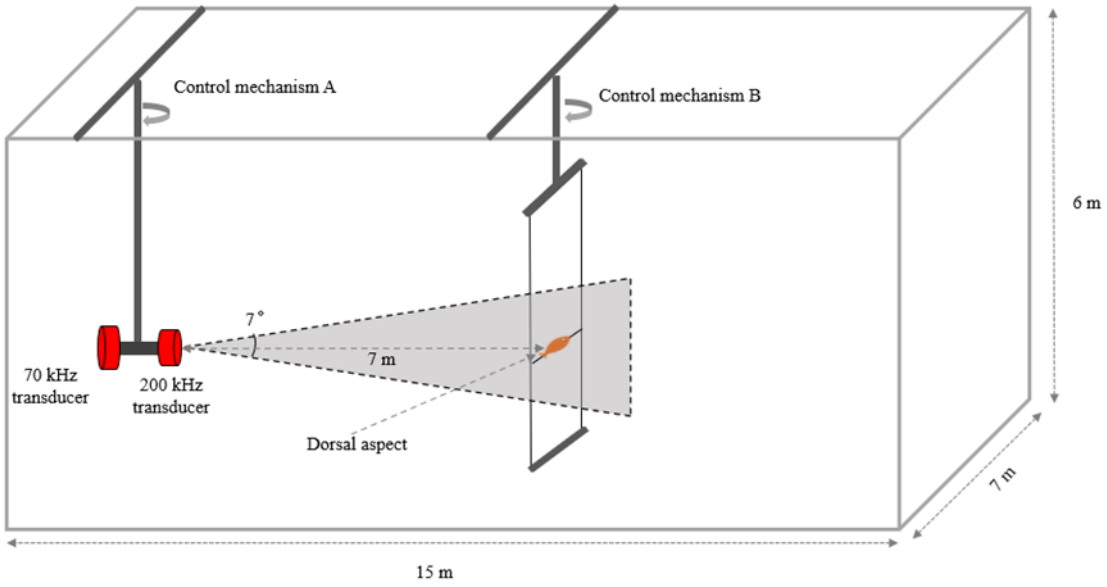

Figure 2. The ex situ TS measurement system. Control mechanism A connects two broadband transducers (center frequency: 70 kHz and 200 kHz), with the gray area representing the beam coverage range. Control mechanism B suspends the fish for measurement, positioning its dorsal side toward the active transducer, while maintaining the fish at the same depth as the transducers.

The Simrad EK80 scientific echosounder system (Kongsberg Maritime AS, Kongsberg, Norway), equipped with two broadband transducers covering frequency from 45 to 90 kHz and 160 to 260 kHz, was used for ex situ TS measurements (Table 2). The two transducers were calibrated using a 38.1 mm diameter tungsten carbide sphere before measurements, following standard methods described by Demer et al. [46]. With reference to the TS spectral response curve of the calibration sphere [47], the frequency bands containing peaks and nulls in the calibration results were excluded from the analysis. Since accurate TS measurements should be taken at least twice the distance beyond the near-field range [48], the near-field ranges corresponding to the two transducers were calculated separately as follows [49]:

$$R = \frac{\pi D^2}{\lambda} \quad (5)$$

where λ is the wavelength (cm) and D is the diameter of the transducer (cm). The transducer calibration and echo data collection were performed using the EK80 software (release V21.15.2, Kongsberg Maritime AS, Kongsberg, Norway) that accompanies the EK80 system.

Table 2. Settings for the EK80 scientific echosounder system.

Parameters	ES70-C	ES200-C
Center frequency (kHz)	70	200
Bandwidth (kHz)	45–90	160–260
Transmitted mode	LFM	LFM
Ramping mode	Fast	Fast
Pulse duration (ms)	1.024	1.024
Sampling frequency (kHz)	62.5	187.5
Beam width (°)	7	7
Transmitted power (W)	750	150
Near-field (m)	2.34	1.07

2.5. Data Analysis

Due to the small sample size and non-normal distribution of the data, we employed the Mann–Whitney U test to compare differences between fish samples measured onboard (before freezing) and those measured by X-ray scans after the survey (after freezing). The Mann–Whitney U test is a non-parametric statistical method used to assess significant differences between two independent groups [50,51]. One advantage of this method is that the two samples do not need to have the same amount of data, and there are no distributional assumptions required that do not assume equal variances between the groups being compared. It is widely applied in diverse fields including medicine, fisheries, and aquaculture [52,53].

To obtain the average TS values of fish targets, the method proposed by Foote [8] was referenced. The average backscattering cross-section (σ_{bs_ave}), which is a linear representation of the average TS, was computed using the Probability Density Function (PDF) of the fish swimming angle distribution by the following:

$$\sigma_{bs\_ave} = \int_{\theta_2}^{\theta_1} \sigma_{bs\_\theta} f(\theta) d\theta \quad (6)$$

$$\mathrm{TS_{ave}} = 10\log_{10} \sigma_{\mathrm{bs\_ave}} \quad (7)$$

Here, θ represents the fish swimming angle, ranging from 40–140°. σ_{bs_θ} represents the backscattering cross-section at angle θ. The fish swimming angle is assumed to follow a normal distribution and $f(\theta)$ represents the PDF of this distribution. In our study, the swimming angle distribution of Chub mackerel was set to $N(93°, 4°)$, as sourced from Nauen et al. [54].

For the KRM model results, the scattering cross-section data can be directly obtained. However, for ex situ TS measurement results, we used the Echoview software (V13.0, Echoview Software Pty Ltd., Tasmania, Australia) to process echo data from the EK80 system. The extraction of TS data at each angle was implemented based on the single target detection-wideband operator provided by the Echoview. The parameter settings are shown in Table 3. The extracted results were then linearly transformed to obtain acoustic scattering cross-section data.

Table 3. Parameters for the single target detection-wideband operator in Echoview.

Parameters	Values	Unit
Operator	Single target detection-wideband	
TS threshold	−80	dB
Pulse length determination level	3/6/9	dB
Minimum normalized pulse length	0.5	
Maximum normalized pulse length	1.5	
Beam compensation model	Simrad Lobe	
Maximum beam compensation	12	dB

In order to investigate the TS characteristics of Chub mackerel, the ratio of the object size to the wavelength was used (L/λ), so that only the effect of changes in acoustic frequency on the TS was considered [55].

Considering that current acoustic estimation of resource abundance still relies mainly on narrowband typical frequencies, the TS–L (body length) relationships were fitted separately using the least-squares method at frequencies of 38 kHz, 70 kHz, 120 kHz, and 200 kHz, referencing empirical formulas [48]:

$$TS = m\log_{10} L + n \tag{8}$$

where m is the slope of the regression, n is the intercept, L is the body length of the fish (cm). The TS of fish with swimbladder is approximately proportional to the square of body length [56], typically with a fixed value of 20 for m, while n is standardized by the square of body length TS_{cm} (b_{20}), as represented by the following equation:

$$TS = 20\log_{10} L + TS_{cm} \tag{9}$$

3. Results

3.1. Swimbladder Morphology and Target Strength Changes before and after Freezing

A total of 37 fresh Chub mackerel samples (before freezing) were dissected and measured for body and swimbladder morphology in the laboratory onboard the research vessel. For the frozen samples, after thorough thawing (about 12 h), X-ray images of 22 Chub mackerel samples were taken and the morphological measurements of the fish body and swimbladder were conducted using Photoshop software. The samples were not the same before and after freezing due to the damage caused by dissection onboard. Both sets of samples were randomly selected.

Before freezing, the length range of samples was 13.3–30.5 cm, with an average length of 18.74 ± 4.22 cm, and the swimbladder length ranged from 3.01 to 7.27 cm, with an average length of 4.62 ± 1.19 cm. For the thawed samples measured, the length range was 14.75–26.93 cm, with average length of 20.51 ± 3.61 cm, the swimbladder length ranged from 2.09 to 7.61 cm, with an average length of 4.79 ± 1.55 cm, and the angle between the swimbladder and the fish body ranged from 6.1 to 13.1°, with an average tilt angle of 10.10 ± 1.19° (Table 4).

To investigate the variations in swimbladder morphology before and after freezing, the percentage of swimbladder relative to corresponding parts of the fish body was calculated. The Mann–Whitney U test was then applied to examine significant differences ($p < 0.05$). The results showed that the proportion of the swimbladder in the fish body decreased after freezing. Specifically, there were significant differences ($p < 0.01$) in the ratio of swimbladder height to body height and swimbladder volume to body volume before and after freezing. This indicated that after freezing, there were significant changes in the swimbladder height and volume relative to the fish body. However, the differences in swimbladder length, width, and dorsal cross-sectional area were not significant.

Table 4. Morphological parameters before and after freezing of Chub mackerel and Mann–Whitney U test.

		Before Freezing (Mean ± sd)	After Freezing (Mean ± sd)	Mann–Whitney U test	
				U	*p*
	No.	**37**	**22**		
fish swimbladder	sbl	4.62 ± 1.19	4.79 ± 1.55		
	sbw	0.99 ± 0.35	1.21 ± 0.30		
	sbh	1.01 ± 0.33	1.00 ± 0.26		
	r	1.65 ± 0.47	0.98 ± 0.23		
	Vsb	2.95 ± 2.67	3.38 ± 2.31		
	Ssb	3.82 ± 2.18	4.73 ± 2.39		
fish body	fbl	18.74 ± 4.22	20.51 ± 3.61		
	fbw	2.21 ± 0.64	2.92 ± 0.69		
	fbh	3.10 ± 0.94	4.02 ± 0.90		
	Vfb	81.83 ± 78.05	141.96 ± 90.15		
	Sfb	34.46 ± 18.99	48.88 ± 19.94		
fish swimbladder to fish body ratio	sbl/fbl	0.25 ± 0.03	0.23 ± 0.05	449	
	sbw/fbw	0.45 ± 0.12	0.42 ± 0.09	436	
	sbh/fbh	0.34 ± 0.10	0.25 ± 0.06	622	***
	Vsb/Vfb	0.04 ± 0.02	0.03 ± 0.01	578	**
	Ssb/Sfb	0.11 ± 0.04	0.10 ± 0.03	508	

Note: **: $p < 0.01$, significant differences; ***: $p < 0.001$, extremely significant differences.

The length, volume, and dorsal cross-sectional area of the swimbladder increased significantly with increasing body length ($p < 0.001$). Before and after freezing, the trends of swimbladder volume and dorsal cross-sectional area increasing with body length are generally consistent, while the trend of swimbladder length increasing with body length is slightly higher after freezing compared to before (Figure 3).

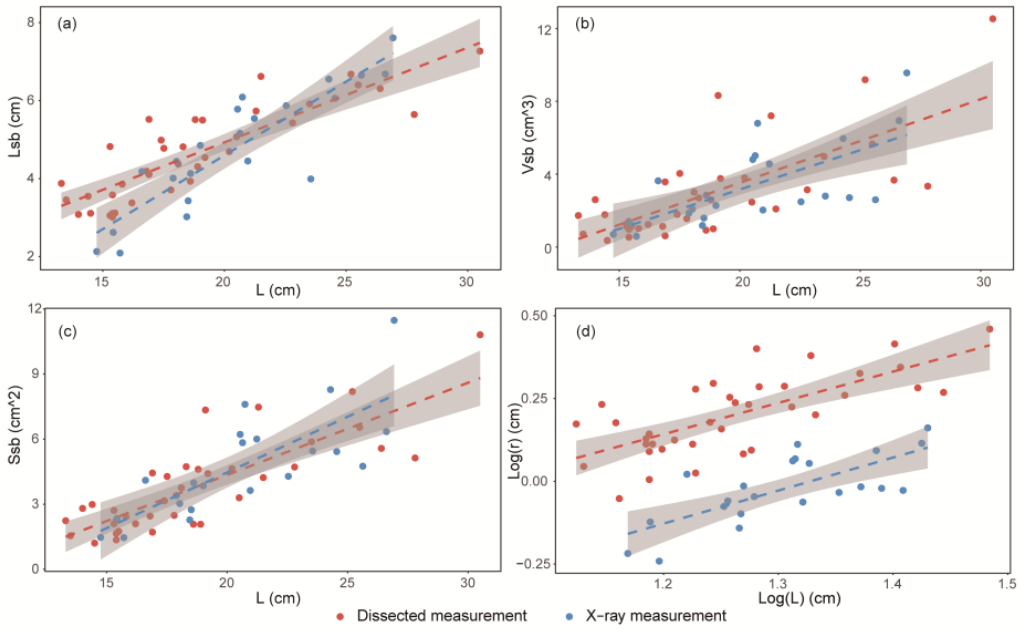

Figure 3. Relationship between the fish body length and the (**a**) swimbladder length, (**b**) swimbladder volume, (**c**) swimbladder cross–sectional area, (**d**) swimbladder equivalent spherical radius. The scatter points represent individual measurements, with red dots indicating fresh sample dissections before freezing and blue dots representing measurements by X-ray after freezing. For all relationships shown in the figures: *p*–value < 0.001.

The logarithmic form of the swimbladder equivalent radius (r) relative to body length can be used to observe the growth trend of the swimbladder. By establishing the following fitting relationships, it was concluded that the allometric exponent of the swimbladder of Chub mackerel before freezing was 0.945, and after freezing was 0.997, indicating that the swimbladder and the body were in a nearly isometric growth state. It is worth noting that the freezing process itself may cause alterations or damage to the swimbladder structure.

Before freezing:

$$\log_{10} r = 0.945 \log_{10} L - 0.992 \quad (10)$$

After freezing:

$$\log_{10} r = 0.997 \log_{10} L - 1.32 \quad (11)$$

Based on post–freezing X-ray imaging data and the differences in swimbladder proportions within the fish body before and after freezing, we used the KRM model to estimate the TS data of 22 fish samples both before and after freezing. The KRM model angle range is 40–140°, and the parameters required for the model, such as those for the fish body, swimbladder, and water, are shown in Table 1. Additionally, the model assumes consistent environmental conditions and homogeneous material properties. As shown in Figure 4, ΔTS represents the difference between the TS before and after freezing. The results showed that despite the reduction in the swimbladder proportion within the fish body due to freezing, the TS did not exhibit a clear trend of increase or decrease at the four typical frequencies of 38, 70, 120, and 200 kHz. The average TS differences at these frequencies were: 0.08 ± 0.19 dB, 0.06 ± 0.30 dB, 0.02 ± 0.78 dB, and 0.23 ± 0.60 dB, respectively. As the frequency increased, the difference in TS before and after freezing gradually became more pronounced, indicating a higher sensitivity of TS changes at higher frequencies.

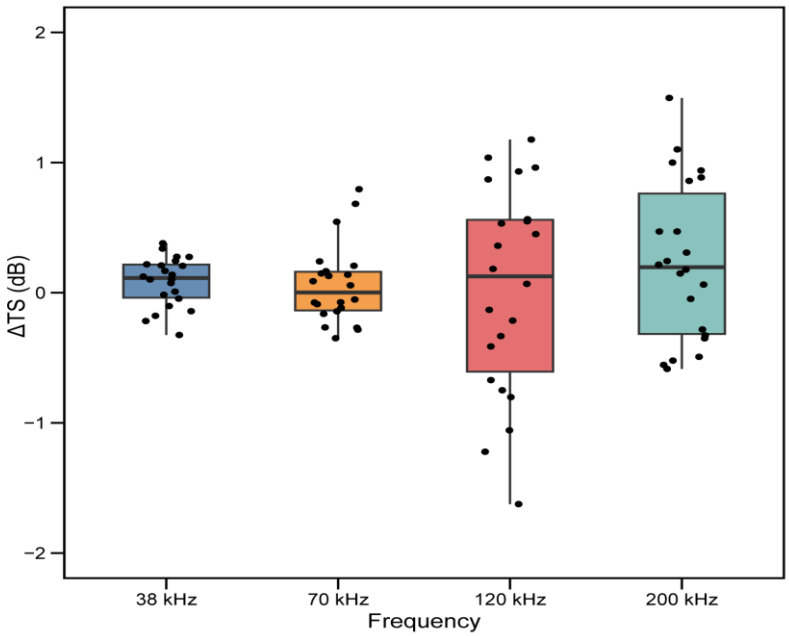

Figure 4. Differences in TS before and after freezing at typical frequencies (38 kHz, 70 kHz, 120 kHz, and 200 kHz) based on the KRM model. ΔTS represents the difference between the TS before and after freezing.

3.2. Comparison of Target Strength between Ex Situ Experiment and KRM Model

Seven individuals were randomly selected from the collected samples (TL: 20.74 ± 1.11 cm) and after thorough thawing for 12 h, KRM model simulation and ex situ TS measurements were conducted to compare the differences between the two methods. X-ray imaging was performed before and after the ex situ measurements to examine the integrity of the swimbladder morphology.

Figure 5 shows the variation in the TS spectra of single Chub mackerel (TL: 21.2 cm) obtained from KRM model simulation and ex situ measurements. Overall, changes in TS relative to angle and frequency were very clearly observed for both measurements. At different frequencies, the maximum TS values were distributed around 100°, when the fish head was away from the transducer and the swimming posture was downward. Combining the measured data of the swimbladder tile angle (10.10° ± 1.49°), the swimbladder was perpendicular to the incident angle of the sound wave, indicating the maximum cross-sectional relative to the sound wave. As frequency increased, the TS exhibited more pronounced directionality. Compared with the regular changes in the TS spectra of the KRM model, the ex situ measurement results showed more heterogeneous TS variations in certain angular intervals.

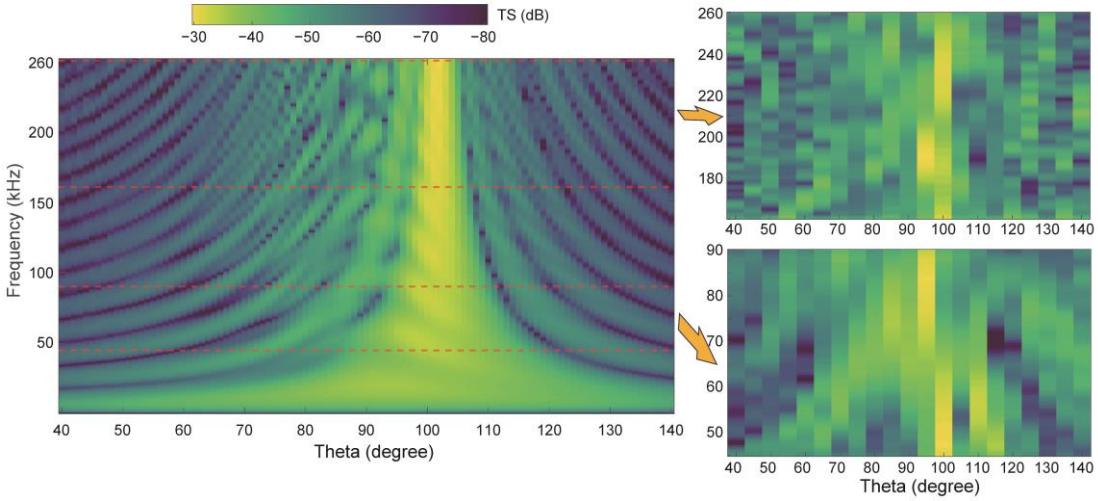

Figure 5. TS variation with angle and frequency for an individual Chub mackerel (body length: 21.2 cm). On the left: the KRM model estimation results, frequency range from 1 to 260 kHz; on the right: ex situ measurement results using broadband transducers for 45–90 kHz and 160–260 kHz frequency ranges. The horizontal axis represents the angle of the fish body relative to the detection beam, ranging from 40 to 140°.

Figure 6 shows the average TS differences of Chub mackerel at various frequencies between the KRM model and ex situ measurements (ΔTS: $TS_{ex\text{-}situ}$–TS_{KRM}), selecting frequency bands within the effective calibration range (45–80 kHz, 180–200 kHz, and 230–240 kHz). The results indicated that the differences between KRM model and ex situ measurements were concentrated within ±3 dB, with an average difference of −0.38 ± 1.84 dB. At the edges of the frequency bands, such as 47 kHz, 80 kHz, 230 kHz, and 233 kHz, larger differences were observed, with some frequencies showing differences exceeding 3 dB, although the larger differences were only found in a single individual case.

3.3. Broadband Scattering Response Characteristics

A total of 22 X-ray scan datasets of Chub mackerel with well-preserved swimbladders were obtained, and the broadband scattering response characteristics were investigated using the KRM model. The average TS of individual fish increased rapidly in the range of approximately 1–30 kHz, which corresponds to the resonance frequency range. Subsequently, as the frequency increased, the change in average TS gradually slowed down and tended to stabilize. There were certain differences in individual TS due to variations in the length of fish samples. By calculating the average TS of all individuals, it was observed that when the frequency exceeded 100 kHz, the average TS remained relatively stable, around −40.76 dB. The maximum TS gradually increased with frequency, and the trend began to stabilize when the frequency reached 150 kHz. As the frequency increased, the difference between the maximum TS and average TS also increased, corresponding to the directional

characteristics of TS. At lower frequencies, the differences in TS between angles were not significant, but as the frequency increased, the directional characteristics of TS became more apparent, leading to larger differences in TS between angles (Figure 7).

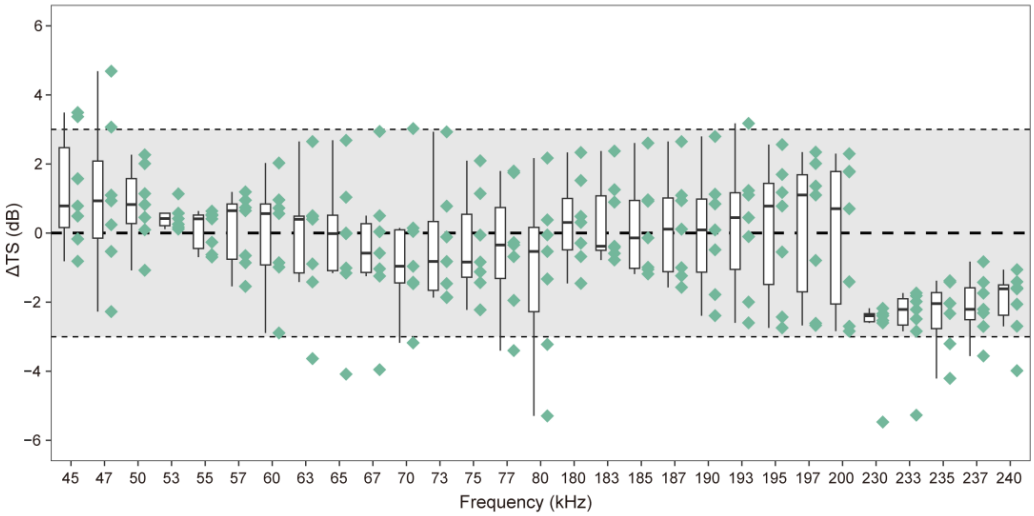

Figure 6. The difference in average TS between Chub mackerel ex situ measurements and KRM model estimates. The horizontal axis represents different frequencies, ranging from 45 to 80 kHz, 180 to 200 kHz, and 230 to 240 kHz. The vertical axis indicates the difference between $TS_{ex\ situ}$ and TS_{KRM}. The shaded area represents the range of ±3 dB.

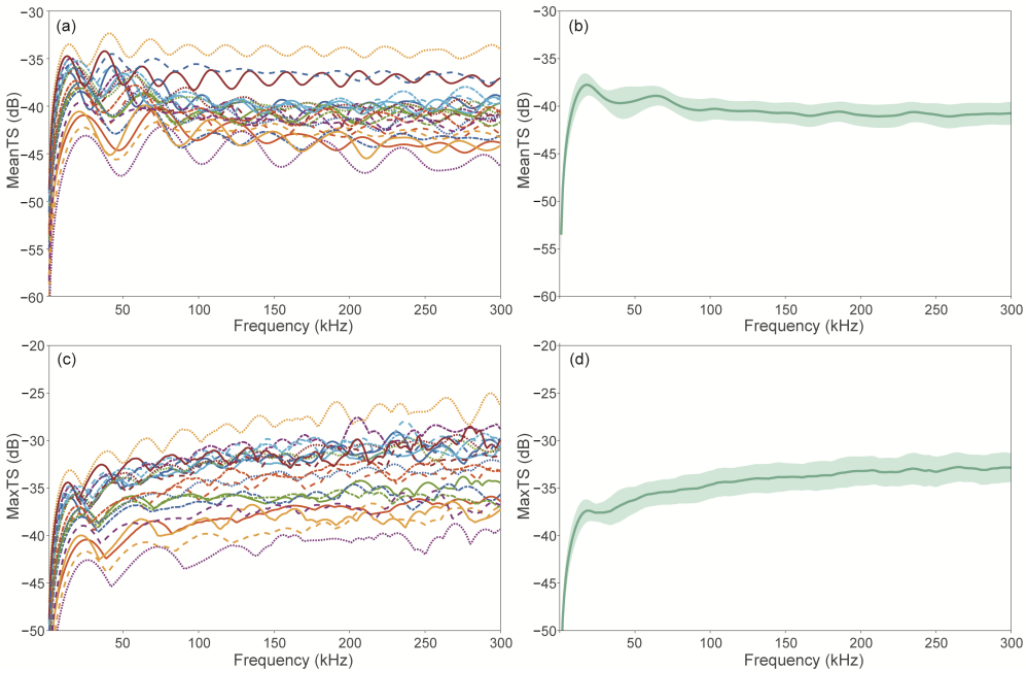

Figure 7. Based on the KRM model results, the average and maximum TS of Chub mackerel vary with frequency: (**a**,**c**) represent the average and maximum TS for different individual fish, with different colored lines representing different individuals; (**b**,**d**) show the average values of average and maximum TS.

We used the ratio of body length (L) to wavelength (λ, c/f) to simultaneously examine the variation of Chub mackerel *TS* with body length and frequency (Figure 8). Within the scope of the study, individual average TScm values were relatively concentrated, fluctuating within a range of about 5 dB, and the fluctuation became smoother as L/λ increased. Then

the TScm of all individuals was averaged, which could reflect the trend of TScm more clearly, and when $L/\lambda > 10$, the TScm basically did not fluctuate. Therefore, the TScm was averaged over all individual TScm in this range ($30 > L/\lambda > 10$) to obtain the relationship between Chub mackerel *TS* and body length under the broadband conditions:

$$TS = 20\log_{10} L - 66.76 \quad (12)$$

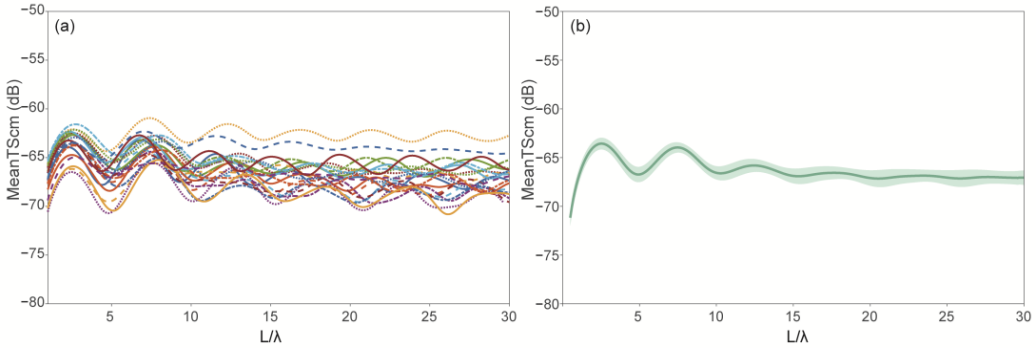

Figure 8. Based on the KRM model results, the relationship between average TScm and L/λ for Chub mackerel: (**a**) represents the average TScm for different individuals of Chub mackerel, with different colored lines representing the variations in TScm among different individuals; (**b**) represents the mean value of average TScm for all individuals of Chub mackerel, with the shaded areas indicating the 95% confidence intervals.

3.4. Relationships between Target Strength and Body Length at Typical Frequencies

Currently, marine fishery resource surveys mainly rely on typical narrowband frequencies such as 38 kHz, 70 kHz, 120 kHz, and 200 kHz. Based on the results of the KRM model, we fitted the TS–L relationships at different typical frequencies to support the acoustic estimation of fishery resources (Figure 9). The specific empirical formulas are as follows.

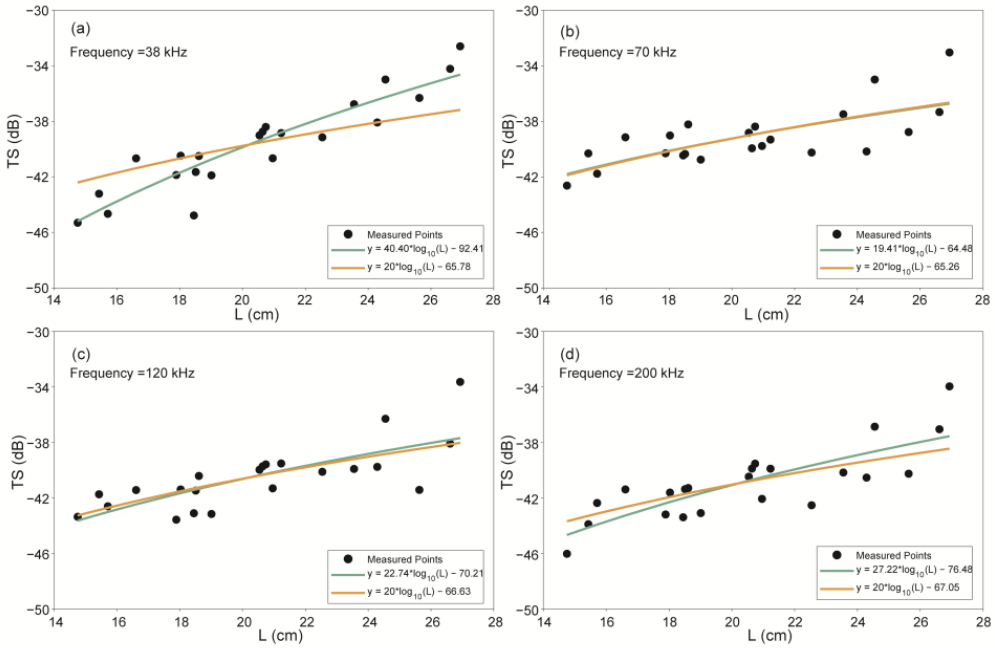

Figure 9. The relationship between TS and body length (L) for Chub mackerel at 38 kHz, 70 kHz, 120 kHz, and 200 kHz derived from the KRM model.

38 kHz:

$$TS = 40.4\log_{10} L - 92.41 \quad (13)$$

(95% CI: m (32.14, 48.65), n (−103.20, −81.62), R^2: 0.84)

$$TS = 20\log_{10} L - 65.78 \quad (14)$$

(95% CI: TScm (−66.70, −64.86), R^2: 0.63)

70 kHz:

$$TS = 19.41\log_{10} L - 64.48 \quad (15)$$

(95% CI: m (10.34, 28.47), n (−76.33, −52.63), R^2: 0.50)

$$TS = 20\log_{10} L - 65.26 \quad (16)$$

(95% CI: TScm (−65.92, −64.59), R^2: 0.50)

120 kHz:

$$TS = 22.74\log_{10} L - 70.21 \quad (17)$$

(95% CI: m (13.18, 32.30), n (−82.72, −57.71), R^2: 0.55)

$$TS = 20\log_{10} L - 66.63 \quad (18)$$

(95% CI: TScm (−67.34, −65.93), R^2: 0.54)

200 kHz:

$$TS = 27.22\log_{10} L - 76.48 \quad (19)$$

(95% CI: m (17.68, 36.76), n (−88.96, −64.01), R^2: 0.64)

$$TS = 20\log_{10} L - 67.05 \quad (20)$$

(95% CI: TScm (−67.79, −66.32), R^2: 0.59)

4. Discussion

In the present study, we measured changes in swimbladder morphology before and after freezing preservation and examined the effects on TS. We compared two common methods for TS research in pelagic fish: ex situ measurements and model estimations, validating the applicability of the KRM model. Based on the KRM, the broadband scattering characteristics of Chub mackerel and the relationship between TS and body length were derived. The results of this study could facilitate species identification and resource assessment of Chub mackerel using acoustic technology, thereby promoting the application of fisheries acoustic technology in the Northwest Pacific Ocean.

For swimbladder-bearing fish, the air stored in the swimbladder creates different media conditions for acoustic pulse transmission, accounting for over 95% of the fish TS [8]. Therefore, studies of TS in swimbladder-bearing fish must consider the effects of the swimbladder. Previous research [12,45] have shown that the variation in fish TS at different angles was consistent with the TS of the swimbladder, with both being very close to each other. The maximum fish TS occurred when the maximum cross-section of the swimbladder was perpendicular to the angle of acoustic incidence. Our results were also consistent with these findings. Additionally, we observed TS characteristics at different angles across successive frequencies and found that TS became more sensitive to angle changes as the frequency increased (Figure 5).

The diel vertical migration (DVM) of small pelagic fish such as Chub mackerel, which accompanies the plankton in the scattering layer, may result in changes in the volume of their swimbladder [57]. When fish ascend, the water pressure decreases, causing the fish to relax and the swimbladder to expand. Conversely, when fish descend, the water pressure increases, causing the fish to tense up and the swimbladder to contract. We considered the changes in swimbladder morphology associated with this fish behavior, and biological

sampling was primarily conducted at night in shallow water layers to minimize changes in swimbladder morphology due to water pressure. Tong et al. [45] used Boyle's law to model the variation of Chub mackerel TS at different depths, but there is a lack of actual data to support the simulation. Future research could consider obtaining live Chub mackerel samples and simulating different water pressure in the laboratory to study changes in the swimbladder volume in different water layers and the effects on TS.

The swimbladder structure of the most economically important pelagic fish is similar to that of the Chub mackerel, with the swimbladder changing according to the depth at which they live, as they are all physostomous fish. In contrast, some mesopelagic and bathypelagic fish, often linked to a deep scattering layer, lack a connection between the swimbladder and the alimentary canal, causing the swimbladder volume to remain constant regardless of water depth [58,59]. Small numbers of epipelagic and demersal fish, including Skipjack tuna (*Katsuwonus pelamis*) and Atlantic mackerel (*Scomber scombrus*), lack a swimbladder. And their acoustic scattering mainly comes from their flesh and backbone, making it much weaker compared to swimbladder-bearing fish [60]. The presence or absence of a swimbladder can be used as a criterion for distinguishing these different marine organisms based on acoustic methods. Although some of these organisms have no global economic value, they are an indispensable part of the marine ecosystem. Separating these from economically significant fisheries resources facilitates the conservation of living marine resources and the maintenance of ecosystems.

Ideally, fresh samples would be preferred for studies of target strength, but this is more challenging for most pelagic organisms. Many studies have used the same method as ours, with rapid freezing in seawater at temperatures below −20 °C. Yasuma et al. [33] pointed out that this procedure has a negligible effect on the swimbladder. However, other studies [61] have indicated that freezing can indeed cause damage to the shape or structure of the fish muscle, which in turn affects the swimbladder. Freezing can also increase the number of bubbles on the surface of the fish, resulting in an increase in TS by 1.9–9.8 dB [62]. There is still a lack of comprehensive research on the effects of different preservation methods on the swimbladder. This study excluded swimbladder changes caused by fish behavior and quantified the effects of seawater freezing preservation on swimbladder morphology. We selected fish individuals that exhibited greater activity and showed no signs of external deformation for sampling. After placing them in seawater for approximately 1 h, we selected samples for dissection or to be frozen, thus minimizing any potential interference with swimbladder morphology during the sampling process. Due to the absence of non-destructive instruments such as X-ray machines on the research vessel, we were unable to compare the same samples before and after freezing. Instead, we minimized potential research errors caused by sample variability by assessing the proportion of swimbladder to different parts of the fish body and employing random sampling. The results showed significant differences in swimbladder height and volume before and after freezing, but those changes did not lead to a consistent increase or decrease in TS. Therefore, we recommend that future research should preferably utilize fresh samples for constructing acoustic models or conducting TS measurements, especially under high-frequency conditions.

By utilizing morphological parameters of fish body and swimbladder, constructing acoustic scattering models for individual fish enables simulation and calculation of TS. This method offers the advantages of flexibility, simplicity in computation, and independence from external environmental constraints. Moreover, with continuous technological advancements, the accuracy of model assessments has improved. Fish TS research based on modeling methods has been applied in various studies on the scattering characteristics of fish both domestically and internationally [26,62,63]. The KRM model, as a physical approximation model, approximates the fish body and swimbladder as multiple contiguous cylinders. It calculates the TS of each individual cylindrical component and then sums them up to obtain the overall TS value of the entire fish [21]. However, fish TS characteristics derived solely from models often require comparison with measurements conducted ex

situ or in situ for validation [12,64]. We compared the KRM model of Chub mackerel with ex situ TS measurement results. When used to study changes in TS at different angles and frequencies, the KRM model not only exhibited significant directional characteristics but also showed more regular TS variations. In contrast, ex situ measurements showed more erratic changes at certain angles. By calculating the average TS at different frequencies, we further demonstrated the applicability of the KRM model in modeling Chub mackerel TS studies. The KRM model assumes that $ka > 0.15$ (where a is the minor radius of a cylinder and k is the wavenumber) for each cylinder derived from the fish body and swimbladder, making the model less accurate when the sound waves are close to the main axis of the fish body [55]. The accuracy of the KRM model is also influenced by the digitization of fish body morphology, including the precision of segmenting the swimbladder and fish body. Additionally, the speed of sound and density values of the fish body, swimbladder, and water are crucial parameters in the KRM model [45]. In our study, we used relevant parameters from a general KRM model for marine fish. It is essential to perform actual measurements of these key parameters in future related experiments to improve the model's accuracy.

In acoustic surveys of fishery resources, obtaining accurate TS–L relationships is crucial for accurately estimating fish stock abundance. In this study, we established empirical relationships between TS and L for Chub mackerel samples with a length range of 14.75–26.93 cm under commonly used fishery survey frequencies. We also compared the previous studies reported in the literature. At the four typical frequencies, the values of TScm were closer to those of Park et al. [23] based on the KRM model (16–28 cm), with differences of 0.24, 1.24, −0.63, and 0.30 dB at each frequency. However, using the same model, the TScm values reported by Tong et al. [45] (12–22 cm) were generally 6–8 dB lower than our results, which may be attributed to differences in body length distribution. Zhu et al. [65] conducted ex situ TS measurements of free-swimming Chub mackerel (17.4–34 cm) in a net cage, and the difference in TScm was 2.12 dB at 38 kHz and 2.57 dB at 120 kHz, which was mainly related to the different angular distributions of the swimming postures, and the TS changes caused by the posture angle were more pronounced with the increase in frequency.

The commercial use of scientific echosounder systems such as the Simrad EK80 system, which simultaneously acquire narrowband and broadband echo data, has shifted research focus toward broadband types [66]. The application of broadband technology in acoustic surveys of fishery resources has become a research hotspot, and studies based on acoustic scattering models can provide reference for species identification based on broadband characteristics. In this study, we utilized the KRM scattering model to construct TS spectral features. Compared to other research, Yan et al. [67] measured the broadband TS of three swimbladder-less fish species, and Lucca et al. [68] measured the broadband TS of various shrimp and shelled pteropods species. These different species exhibited distinct spectral characteristics, and these differences are key to species identification based on broadband acoustic technology.

Our study has several limitations: Firstly, the samples measured before and after freezing were not the same individuals, and the sample sizes differed, which may lead to uncertainties in TS changes. Secondly, different methods were used for measuring the swimbladder, which introduces uncertainties in TS changes based on these differences. The parameters used in the KRM model were mainly derived from previous literature, without on-site measurements. Additionally, the sample size was limited, and the geographic scope was narrow. To address these issues, we plan to use the same batch and a consistent number of samples for pre- and post-freezing comparisons in future research, adopt consistent methods for measuring the swimbladder, and conduct on-site parameter measurements. Furthermore, we will increase the geographic range of our samples to improve the applicability of our results. We believe that addressing these limitations will enhance the contribution of our study to marine acoustic research.

5. Conclusions

This study investigated the impact of freezing preservation on the swimbladder morphology and the TS of Chub mackerel, and compared two methods for TS estimation, then examined the broadband scattering characteristics. Our findings indicated that freezing preservation leads to significant changes in swimbladder morphology, notably in its height and volume. However, these morphological changes do not result in consistent and significant variations in TS. The comparison between the KRM model and ex situ TS measurements revealed a good agreement, with differences concentrated within ± 3 dB and an average difference of -0.38 ± 1.84 dB. This validated the applicability of the KRM model for TS estimation of Chub mackerel under various conditions. Based on the KRM results, the TS of Chub mackerel exhibited significant directivity, with fluctuations gradually decreasing and stabilizing as frequency increased. In the broadband mode, the relationship between TS and body length (L) of Chub mackerel was TS = 20log(L)−66.76 ($30 > L/\lambda > 10$). Our research could provide essential data for acoustic resource estimation and species identification.

Author Contributions: Conceptualization, Z.Z.; Funding acquisition, B.L.; Methodology, Z.Z., J.T., and M.X.; Project administration, J.T. and B.L.; Software, Z.Z., M.X., C.Q., and S.L.; Supervision, J.T.; Writing—original draft, Z.Z.; Writing—review and editing, J.T. All authors have read and agreed to the published version of the manuscript.

Funding: This research was funded by the National Key R&D Program of China (2023YFD2401302, 2019YFD0901401). We also acknowledge funds provided by the Ministry of Agriculture and Rural Affairs of China through the project on the Survey and Monitor-Evaluation of Global Fishery Resources.

Institutional Review Board Statement: The study was approved by the Shanghai Ocean University Scientific Research Department (Approval code: SHOU-DW-2023-097).

Informed Consent Statement: Not applicable.

Data Availability Statement: Data will be made available on request.

Acknowledgments: The authors of this research would like to thank all the researchers and sailors on RV Songhang, especially Shujie Wan and Hao Xv, who contributed to the data collection during the marine survey. Special thanks to the Fishery Machinery and Instrument Research Institute, Chinese Academy of Fishery Sciences, for providing experimental site support. Thanks to the Institute of Hydroecology, MWR, and CAS for providing equipment support. Thanks to the reviewers for the thoughtful discussion that substantially improved the original manuscript.

Conflicts of Interest: The authors declare no conflicts of interest.

References

1. Andersen, L.N.; Chu, D.; Handegard, N.O.; Heimvoll, H.; Korneliussen, R.; Macaulay, G.J.; Ona, E.; Patel, R.; Pedersen, G. Quantitative Processing of Broadband Data as Implemented in a Scientific Split-Beam Echosounder. *Methods Ecol. Evol.* **2024**, *15*, 317–328. [CrossRef]
2. Palermino, A.; De Felice, A.; Canduci, G.; Biagiotti, I.; Costantini, I.; Centurelli, M.; Leonori, I. Application of an Analytical Approach to Characterize the Target Strength of Ancillary Pelagic Fish Species. *Sci. Rep.* **2023**, *13*, 15182. [CrossRef] [PubMed]
3. Sun, M.; Cai, Y.; Zhang, K.; Zhao, X.; Chen, Z. A Method to Analyze the Sensitivity Ranking of Various Abiotic Factors to Acoustic Densities of Fishery Resources in the Surface Mixed Layer and Bottom Cold Water Layer of the Coastal Area of Low Latitude: A Case Study in the Northern South China Sea. *Sci. Rep.* **2020**, *10*, 11128. [CrossRef] [PubMed]
4. Simmonds, J.; MacLennan, D.N. *Fisheries Acoustics: Theory and Practice*; John Wiley & Sons: Hoboken, NJ, USA, 2008.
5. Stanton, T.K.; Sellers, C.J.; Jech, J.M. Resonance Classification of Mixed Assemblages of Fish with Swimbladders Using a Modified Commercial Broadband Acoustic Echosounder at 1–6 kHz. *Can. J. Fish. Aquat. Sci.* **2012**, *69*, 854–868. [CrossRef]
6. Andersen, L.N.; Chu, D.; Heimvoll, H.; Korneliussen, R.; Macaulay, G.J.; Ona, E. Quantitative Processing of Broadband Data as Implemented in a Scientific Splitbeam Echosounder. *arXiv* **2021**, arXiv:2104.07248. [CrossRef]
7. Yamamoto, N.; Amakasu, K.; Abe, K.; Matsukura, R.; Imaizumi, T.; Matsuura, T.; Murase, H. Volume Backscattering Spectra Measurements of Antarctic Krill Using a Broadband Echosounder. *Fish. Sci.* **2023**, *89*, 301–315. [CrossRef]
8. Foote, K.G. Importance of the Swimbladder in Acoustic Scattering by Fish: A Comparison of Gadoid and Mackerel Target Strengths. *J. Acoust. Soc. Am.* **1980**, *67*, 2084–2089. [CrossRef]

9. Hazen, E.L.; Horne, J.K. A Method for Evaluating the Effects of Biological Factors on Fish Target Strength. *ICES J. Mar. Sci.* **2003**, *60*, 555–562. [CrossRef]
10. Lu, H.-J.; Kang, M.; Huang, H.-H.; Lai, C.-C.; Wu, L.-J. Ex Situ and in Situ Measurements of Juvenile Yellowfin Tuna Thunnus Albacares Target Strength. *Fish. Sci.* **2011**, *77*, 903–913. [CrossRef]
11. Pérez-Arjona, I.; Godinho, L.; Espinosa, V. Influence of Fish Backbone Model Geometrical Features on the Numerical Target Strength of Swimbladdered Fish. *ICES J. Mar. Sci.* **2020**, *77*, 2870–2881. [CrossRef]
12. Madirolas, A.; Membiela, F.A.; Gonzalez, J.D.; Cabreira, A.G.; dell'Erba, M.; Prario, I.S.; Blanc, S. Acoustic Target Strength (TS) of Argentine Anchovy (*Engraulis Anchoita*): The Nighttime Scattering Layer. *ICES J. Mar. Sci.* **2017**, *74*, 1408–1420. [CrossRef]
13. Li, B.; Liu, J.; Gao, X.; Huang, H.; Wang, F.; Huang, Z. Acoustic Target Strength of Thornfish (*Terapon jarbua*) Based on the Kirchhoff-Ray Mode Model. *Electronics* **2024**, *13*, 1279. [CrossRef]
14. Horne, J.K. Acoustic Approaches to Remote Species Identification: A Review. *Fish. Oceanogr.* **2000**, *9*, 356–371. [CrossRef]
15. Sobradillo, B.; Boyra, G.; Martinez, U.; Carrera, P.; Peña, M.; Irigoien, X. Target Strength and Swimbladder Morphology of Mueller's Pearlside (*Maurolicus muelleri*). *Sci Rep.* **2019**, *9*, 17311. [CrossRef] [PubMed]
16. Boyra, G.; Moreno, G.; Orue, B.; Sobradillo, B.; Sancristobal, I. In Situ Target Strength of Bigeye Tuna (*Thunnus obesus*) Associated with Fish Aggregating Devices. *ICES J. Mar. Sci.* **2019**, *76*, 2446–2458. [CrossRef]
17. Hasegawa, K.; Yan, N.; Mukai, T. In Situ Broadband Acoustic Measurements of Age-0 Walleye Pollock and Pointhead Flounder in Funka Bay, Hokkaido, Japan. *J. Mar. Sci. Technol.* **2021**, *29*, 135–145. [CrossRef]
18. Kang, D.; Cho, S.; Lee, C.; Myoung, J.-G.; Na, J. Ex Situ Target-Strength Measurements of Japanese Anchovy (*Engraulis japonicus*) in the Coastal Northwest Pacific. *ICES J. Mar. Sci.* **2009**, *66*, 1219–1224. [CrossRef]
19. Kim, H.; Cho, S.; Kim, M.; Kim, S.; Kang, D. Acoustic Target Strength According to Different Growth Stages of Japanese Anchovy (*Engraulis japonicus*): A Comparison of Juvenile and Adult Fish. *J. Mar. Sci. Eng.* **2023**, *11*, 1575. [CrossRef]
20. Yoon, E.; Lee, H.; Park, C.; Lee, Y.-D.; Hwang, K.; Kim, D.N. Ex Situ Target Strength of Yellow Croaker (*Larimichthys polyactis*) in a Seawater Tank. *Fish. Res.* **2023**, *260*, 106610. [CrossRef]
21. Macaulay, G.J.; Pena, H.; Fassler, S.M.M.; Pedersen, G.; Ona, E. Accuracy of the Kirchhoff-Approximation and Kirchhoff-Ray-Mode Fish Swimbladder Acoustic Scattering Models. *PLoS ONE* **2013**, *8*, e64055. [CrossRef] [PubMed]
22. Bonomo, A.L.; Isakson, M.J. Modeling the Acoustic Scattering from Axially Symmetric Fluid, Elastic, and Poroelastic Objects Due to Nonsymmetric Forcing Using COMSOL Multiphysics. In Proceedings of the 2016 COMSOL Conference, Boston, MA, USA, 5–7 October 2016.
23. Park, G.; Oh, W.; Oh, S.; Lee, K. Acoustic scattering characteristics of chub mackerel (*Scomber japonicus*) by KRM model. *J. Korean Soc. Fish. Technol.* **2022**, *58*, 32–38. [CrossRef]
24. Sawada, K.; Takahashi, H.; Abe, K.; Ichii, T.; Watanabe, K.; Takao, Y. Target-Strength, Length, and Tilt-Angle Measurements of Pacific Saury (*Cololabis saira*) and Japanese Anchovy (*Engraulis japonicus*) Using an Acoustic-Optical System. *ICES J. Mar. Sci.* **2009**, *66*, 1212–1218. [CrossRef]
25. Pérez-Arjona, I.; Godinho, L.; Espinosa, V. Numerical Simulation of Target Strength Measurements from near to Far Field of Fish Using the Method of Fundamental Solutions. *Acta Acust. United Acust.* **2018**, *104*, 25–38. [CrossRef]
26. Yang, H.; Cheng, J.; Tang, T.; Chen, J.; Li, G. Acoustic Target Strength of Jellyfish, *Nemopilema nomurai*, Measured at Multi-Frequency and Multi-Orientation. *J. Appl. Ichthyol.* **2023**, *2023*, 6650863. [CrossRef]
27. Jech, J.M.; Horne, J.K.; Chu, D.; Demer, D.A.; Francis, D.T.; Gorska, N.; Jones, B.; Lavery, A.C.; Stanton, T.K.; Macaulay, G.J. Comparisons among Ten Models of Acoustic Backscattering Used in Aquatic Ecosystem Research. *J. Acoust. Soc. Am.* **2015**, *138*, 3742–3764. [CrossRef] [PubMed]
28. Hazen, E.L.; Horne, J.K. Comparing the Modelled and Measured Target-Strength Variability of Walleye Pollock, *Theragra chalcogramma*. *ICES J. Mar. Sci.* **2004**, *61*, 363–377. [CrossRef]
29. Peña, H.; Foote, K.G. Modelling the Target Strength of *Trachurus symmetricus* Murphyi Based on High-Resolution Swimbladder Morphometry Using an MRI Scanner. *ICES J. Mar. Sci.* **2008**, *65*, 1751–1761. [CrossRef]
30. Sawada, K.; Uchikawa, K.; Matsuura, T.; Sugisaki, H.; Amakasu, K.; Abe, K. In Situ and Ex Situ Target Strength Measurement of Mesopelagic Lanternfish, Diaphus Theta (Family *Myctophidae*). *J. Mar. Sci. Technol.* **2011**, *19*, 10. [CrossRef]
31. Sobradillo, B.; Boyra, G.; Pérez-Arjona, I.; Martinez, U.; Espinosa, V. Ex Situ and in Situ Target Strength Measurements of European Anchovy in the Bay of Biscay. *ICES J. Mar. Sci.* **2021**, *78*, 782–796. [CrossRef]
32. Yasuma, H.; Sawada, K.; Ohshima, T.; Miyashita, K.; Aoki, I. Target Strength of Mesopelagic Lanternfishes (Family *Myctophidae*) Based on Swimbladder Morphology. *ICES J. Mar. Sci.* **2003**, *60*, 584–591. [CrossRef]
33. Yasuma, H.; Sawada, K.; Takao, Y.; Miyashita, K.; Aoki, I. Swimbladder Condition and Target Strength of Myctophid Fish in the Temperate Zone of the Northwest Pacific. *ICES J. Mar. Sci.* **2010**, *67*, 135–144. [CrossRef]
34. FAO. *The State of World Fisheries and Aquaculture*; Food & Agriculture Organization: Rome, Italy, 2022; Volume 3.
35. Cai, K.; Kindong, R.; Ma, Q.; Tian, S. Stock Assessment of Chub Mackerel (*Scomber japonicus*) in the Northwest Pacific Using a Multi-Model Approach. *Fishes* **2023**, *8*, 80. [CrossRef]
36. NPFC Secretariat. Summary Footprint of Chub Mackerel Fisheries. NPFC-2023-AR-Annual Summary Footprint. 2023. Available online: https://www.npfc.int/summary-footprint-chub-mackerel-fisheries (accessed on 1 May 2024).
37. Shi, Y.; Zhang, X.; He, Y.; Fan, W.; Tang, F. Stock Assessment Using Length-Based Bayesian Evaluation Method for Three Small Pelagic Species in the Northwest Pacific Ocean. *Front. Mar. Sci.* **2022**, *9*, 775180. [CrossRef]

38. Sogawa, S.; Hidaka, K.; Kamimura, Y.; Takahashi, M.; Saito, H.; Okazaki, Y.; Shimizu, Y.; Setou, T. Environmental Characteristics of Spawning and Nursery Grounds of Japanese Sardine and Mackerels in the Kuroshio and Kuroshio Extension Area. *Fish Oceanogr.* **2019**, *28*, 454–467. [CrossRef]
39. Xue, M.; Tong, J.; Tian, S.; Wang, X. Broadband Characteristics of Zooplankton Sound Scattering Layer in the Kuroshio–Oyashio Confluence Region of the Northwest Pacific Ocean in Summer of 2019. *J. Mar. Sci. Een.* **2021**, *9*, 938. [CrossRef]
40. Zhu, Z.; Tong, J.; Xue, M.; Sarr, O.; Gao, T. Assessing the Influence of Abiotic Factors on Small Pelagic Fish Distribution across Diverse Water Layers in the Northwest Pacific Ocean through Acoustic Methods. *Eco. Indic.* **2024**, *158*, 111563. [CrossRef]
41. Sarmiento-Lezcano, A.N.; Pilar Olivar, M.; Jose Caballero, M.; Couret, M.; Hernandez-Leon, S.; Castellon, A.; Pena, M. Swimbladder Properties of *Cyclothone* spp. in the Northeast Atlantic Ocean and the Western Mediterranean Sea. *Front. Mar. Sci.* **2023**, *10*, 1093982. [CrossRef]
42. Saenger, R.A. Bivariate Normal Swimbladder Size Allometry Models and Allometric Exponents for 38 Mesopelagic Swimbladdered Fish Species Commonly Found in the North Sargasso Sea. *Can. J. Fish. Aquat. Sci.* **1989**, *46*, 1986–2002. [CrossRef]
43. Clay, C.S.; Horne, J.K. Acoustic Models and Target Strengths of the Atlantic Cod (*Gadus morhua*). *JASA* **1992**, *92*, 2350–2351. [CrossRef]
44. Clay, C.S.; Horne, J.K. Acoustic Models of Fish: The Atlantic Cod (*Gadus morhua*). *JASC* **1994**, *96*, 1661–1668. [CrossRef]
45. Tong, J.; Xue, M.; Zhu, Z.; Wang, W.; Tian, S. Impacts of Morphological Characteristics on Target Strength of Chub Mackerel (*Scomber japonicus*) in the Northwest Pacific Ocean. *Front. Mar. Sci.* **2022**, *9*, 10. [CrossRef]
46. Demer, D.A.; Berger, L.; Bernasconi, M.; Bethke, E.; Boswell, K.; Chu, D.; Domokos, R.; Dunford, A.; Fassler, S.; Gauthier, S.; et al. Calibration of Acoustic Instruments; ICES: 2015. Available online: https://repository.oceanbestpractices.org/handle/11329/626 (accessed on 30 May 2024).
47. Simrad. *Simrad EK80 Wide Band Scientific Echo Sounder Reference Manual, Release: 21.15; Kongsberg Maritime AS., Kongsberg, Norway*. 2022. Available online: https://www.kongsbergdiscovery.net/ek80/documents.htm (accessed on 15 May 2024).
48. MacLennan, D.N.; Simmonds, E.J. *Fisheries Acoustics*; Springer Science & Business Media: Berlin/Heidelberg, Germany, 2013; Volume 5, ISBN 94-017-1558-0.
49. Urick, R.J. *Principles of Underwater Sound*; McGraw-Hill Book Co.: New York, NY, USA, 1983.
50. Hart, A. Mann-Whitney Test Is Not Just a Test of Medians: Differences in Spread Can Be Important. *BMJ* **2001**, *323*, 391–393. [CrossRef] [PubMed]
51. Swathi Lekshmi, P.S.; Radhakrishnan, K.; Narayanakumar, R.; Vipinkumar, V.P.; Parappurathu, S.; Salim, S.S.; Johnson, B.; Pattnaik, P. Gender and Small-Scale Fisheries: Contribution to Livelihood and Local Economies. *Mar. Policy* **2021**, *136*, 104913. [CrossRef]
52. Pérez, N.P.; Guevara López, M.A.; Silva, A.; Ramos, I. Improving the Mann–Whitney Statistical Test for Feature Selection: An Approach in Breast Cancer Diagnosis on Mammography. *Artif. Intell. Med.* **2015**, *63*, 19–31. [CrossRef] [PubMed]
53. Sanyé-Mengual, E.; Specht, K.; Krikser, T.; Vanni, C.; Pennisi, G.; Orsini, F.; Gianquinto, G.P. Social Acceptance and Perceived Ecosystem Services of Urban Agriculture in Southern Europe: The Case of Bologna, Italy. *PLoS ONE* **2018**, *13*, e0200993. [CrossRef] [PubMed]
54. Nauen, J.C.; Lauder, G.V. Hydrodynamics of Caudal Fin Locomotion by Chub Mackerel, *Scomber japonicus* (*Scombridae*). *J. Exp. Biol.* **2002**, *205*, 1709–1724. [CrossRef] [PubMed]
55. Yang, Y.; Gastauer, S.; Proud, R.; Mangeni-Sande, R.; Everson, I.; Kayanda, R.J.; Brierley, A.S. Modelling and in Situ Observation of Broadband Acoustic Scattering from the Silver Cyprinid (*Rastrineobola argentea*) in Lake Victoria, East Africa. *ICES J. Mar. Sci.* **2023**, 1–14. [CrossRef]
56. Furusawa, M.; Miyanohana, Y. Application of Echo-Trace Analysis to Estimation of Behaviour and Target Strength of Fish. *Acoust. Sci. Technol.* **1988**, *9*, 169–180. [CrossRef]
57. Kanwisher, J.; Ebeling, A. Composition of the Swim-Bladder Gas in Bathypelagic Fishes. *Deep. Sea Res.* **1957**, *4*, 211–217. [CrossRef]
58. Benoit-Bird, K.J.; Au, W.W.; Kelley, C.D.; Taylor, C. Acoustic Backscattering by Deepwater Fish Measured in Situ from a Manned Submersible. *Deep. Sea Res. Part I Oceanogr. Res. Pap.* **2003**, *50*, 221–229. [CrossRef]
59. Albano, M.; D'iglio, C.; Spanò, N.; Fernandes, J.M.d.O.; Savoca, S.; Capillo, G. Distribution of the Order Lampriformes in the Mediterranean Sea with Notes on Their Biology, Morphology, and Taxonomy. *Biology* **2022**, *11*, 1534. [CrossRef] [PubMed]
60. Ladino, A.; Pérez-Arjona, I.; Espinosa, V.; Chillarón, M.; Vidal, V.; Godinho, L.M.; Boyra, G. Role of material properties in acoustical target strength: Insights from two species lacking a swimbladder. *Fish. Res.* **2024**, *270*, 106895. [CrossRef]
61. Rumape, O.; Elveny, M.; Suksatan, W.; Hatmi, R.U.; Voronkova, O.Y.; Bokov, D.O.; Wanita, Y.P. Study on the quality of fish products based on different preservation techniques: A review. *Food Sci. Technol.* **2022**, *42*, e78521. [CrossRef]
62. Yoon, E.; Oh, W.-S.; Lee, H.; Hwang, K.; Kim, D.-N.; Lee, K. Comparison of Target Strength of Pacific Herring (*Clupea pallasii* Valenciennes, 1847) from Ex-Situ Measurements and a Theoretical Model. *Water* **2021**, *13*, 3009. [CrossRef]
63. Sathish, K.; Anbazhagan, R.; Venkata, R.C.; Arena, F.; Pau, G. Investigation and Numerical Simulation of the Acoustic Target Strength of the Underwater Submarine Vehicle. *Inventions* **2022**, *7*, 111. [CrossRef]
64. Fässler, S.M.; O'Donnell, C.; Jech, J.M. Boarfish (*Capros aper*) Target Strength Modelled from Magnetic Resonance Imaging (MRI) Scans of Its Swimbladder. *ICES J. Mar. Sci.* **2013**, *70*, 1451–1459. [CrossRef]

65. Zhu, Y.; Mizutani, K.; Minami, K.; Shirakawa, H.; Kawauchi, Y.; Shao, H.; Tomiyasu, M.; Iwahara, Y.; Tamura, T.; Ogawa, M.; et al. Target Strength Measurements of Free-Swimming Sandeel Species, Ammodytes Spp., in a Large Indoor Experimental Aquarium. *J. Mar. Sci. Eng.* **2022**, *10*, 966. [CrossRef]
66. McClatchie, S.; Macaulay, G.; Coombs, R.F.; Grimes, P.; Hart, A. Target Strength of an Oily Deep-Water Fish, Orange Roughy (*Hoplostethus atlanticus*) I. Experiments. *JASA* **1999**, *106*, 131–142. [CrossRef]
67. Yan, N.; Mukai, T.; Hasegawa, K.; Yamamoto, J.; Fukuda, Y. Broadband target strength of arabesque greenling, Pacific sand lance, and pointhead flounder. *ICES J. Mar. Sci.* **2023**, *81*, 195–203. [CrossRef]
68. Lucca, B.M.; Warren, J.D. Experimental target strength measurements of pteropods and shrimp emphasize the importance of scattering model inputs. *ICES J. Mar. Sci.* **2024**, fsad211. [CrossRef]